

Design of A Close-range Radiotherapy Particle Implantation Device*

Guang Ban, Changle Li, Xuehe Zhang, Gangfeng Liu, Yubin Liu,

Jie Zhao, Leifeng Zhang and Yilun Fan

State Key Laboratory of Robotics and System

Harbin Institute of Technology

Harbin 150080, NO. 2, YiKuang Street, NanGang District Harbin City, HeiLongJiang Province, China

19S008048@stu.hit.edu.cn

{lichangle, zhangxuehe, liugangfeng, liuyubin & jzhao}@hit.edu.cn

leifeng_zhang@yeah.net, 1246371494@qq.com

Abstract - The validity of brachytherapy has been proved in clinical tumor treatment, and robotic surgery system has been used in recent years to ensure surgical consistency. In our work, a new automatic radioactive particle implantation device with two degrees of freedom was proposed to apply in the brachytherapy robotic surgery system as an end effector. Furthermore, physical assembling and simple function verifying experiments were accomplished. This device can help simplify the operating steps during surgery, and improve the stability of the surgical system, and enhances the surgical efficiency.

Index Terms - Surgical robot, Internal radiation, Particle implantation device, Puncture surgery.

I. INTRODUCTION

In recent years, brachytherapy has been proved effective in the minimally invasive treatment of malignant tumors and has been widely used in the treatment of breast cancer, lung cancer and prostate cancer. The principle of brachytherapy is to implant the radioactive particles into the tumor or the infiltrated tissue near the tumor through puncture needle, under the guidance of medical image including CT and ultrasound, so that the radiation released by the decaying process of the radioactive particles kills the tumor cells.

The use of robotic surgery system can tackle the issues including: 1. Brachytherapy requires experienced doctor. 2. Human hands tremors introduce error to surgical operations. 3. Radiation exposure of medical care personnel and the patient. It is very important to improve the particle implantation accuracy which is mainly determined by the positioning accuracy of the robot and the puncture accuracy of the end effector.

In 2007, H. Bassan and T. Hayes of Western Ontario University in Canada developed a microscopic percutaneous puncture needle system based on 3D ultrasound navigation. The system is mainly composed of a micro needle mechanism, a 2D ultrasound probe, an ultrasound imaging device and an industrial computer. The micro-needle mechanism has a total of 5 degrees of freedom, in which there are two degrees of freedom of rotation and translation in the insertion direction of the needle body, so the mechanism can skillfully insert and rotate the needle body, and use a linear motor to rotate the columnar ultrasonic probe. Accurately placed near the target, using agar as the experimental object, verified that the robot's needle error was 1.45mm. The disadvantage is that the structure is too complicated, the device is bulky, and the manufacturing cost is high.

In 2009, Hungr developed the GHUG ultrasonic navigation particle robot system. The system includes a positioning module and a needle insertion module. In order to improve the precision of the needling, the rotation degree of the needle is increased in the needle insertion module, and low-dose particle implantation can be performed. Into the surgery. However, the implant dose of this device is limited.

In 2016, Zhang Yongde and others of Harbin University of Science and Technology designed a multi-channel prostate short-range radioactive particle implant device, which consists of a two-way moving mechanism, a position adjustment mechanism, an electric particle implantation mechanism and a multi-channel puncture mechanism. Multi-channel external needle implantation is realized, but the external needle implantation angle is limited, the device is bulky, and the

* This work is supported by the National Natural Science Foundation of China (NSFC) (Grant no. U1713202, 61803126), National High-tech R&D Program of China (No. 2017YFB1303600) and DongGuan Major Special Project (no. 201721502011).

particles still need to be manually placed and injected by a doctor.

In 2017, Duan Xingguang and Chen Ningning of Beijing Institute of Technology conducted the design of particle storage and automatic implant device in the design of radioactive particle implantation robot for craniofacial tumor. The mechanism consists of a particle storage device, a medical particle implant needle, a stepping motor and a holding mechanism. However, the end device is not flexible enough to achieve one degree of freedom of needle advancement, and the external needle puncture still relies entirely on the robot arm, and the puncture accuracy depends on the accuracy of the robot arm. Moreover, the particle storage device is too large, and the structural layout of the device is not coordinated enough.

In our work, we propose a new automatic radioactive particle implantation device with two degrees of freedom that can improve puncture accuracy of the end effector, therefore improve the stability of the whole system.

OUTLINE: The designing idea and detail is shown in part II, structural strength check result is represented in part III. We designed the control system of the device to manifest the puncture process, both the hardware and software are introduced in part IV. At last in part V, we accomplished the manufacturing and assembling, and did several function verifying experiments.

II. STRUCTURAL DESIGNING

A. Requirements Analysis

The device is designed according to the existing puncture needle and hand operating procedure of brachytherapy surgery, and the required action procedures are shown in fig.1:

1) The outer needle is inserted into the body at a specified depth (in the vicinity of the tumor cell).

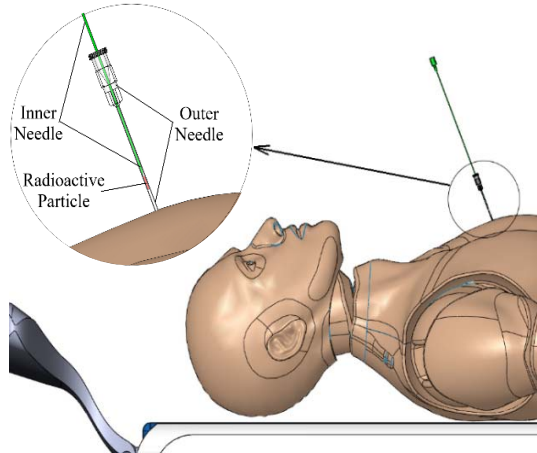


Fig. 1 Particle implantation process

- 2) A $\varnothing 0.8$ specification of radioactive particle is automatically added to the outer needle core.
- 3) The inner needle advances the particle injection near the tumor cells.
- 4) Repeat steps 2) and 3) to inject the required number of particles.
- 5) Adjust the depth of the outer needle and continue step 4).

About 30 to 50 radioactive particles need to be implanted for each operation.

After preliminary analysis of the required action procedures, it is concluded that three mechanisms need to be designed: The External Needle Insertion Mechanism, The Automatic Particle Placement Mechanism, and The Internal Needle Repeated Injection Mechanism.

B. Mechanisms Structural Design

The implantation device consists of 3 parts, namely: Part 1. The external needle insertion mechanism. Part 2. The automatic particle placement mechanism. Part 3. The internal needle reciprocating propulsion mechanism.

Figs. 2 shows three-dimensional model of the device. After the structural design is completed, in order to ensure the visibility of the device and the protection of the transmission mechanism and the like, the shell design of the device is finally added. Figs. 3 and 4 exhibit front and top views of the device.

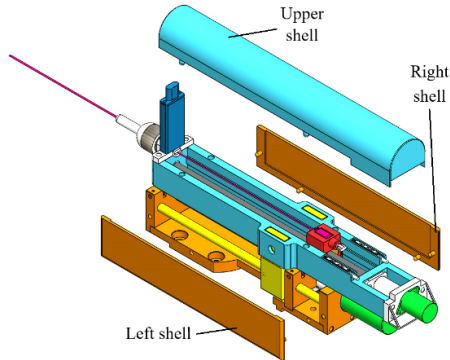


Fig. 2 Three-dimensional model of the device

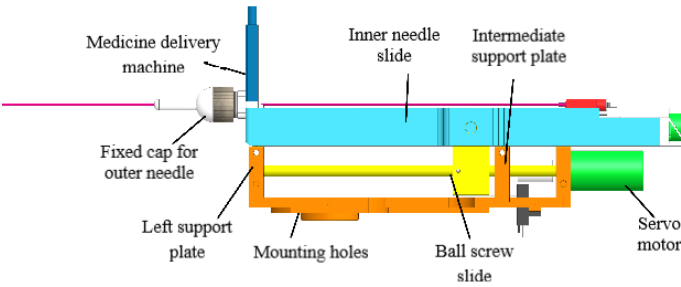


Fig. 3 Front view of the assembly.

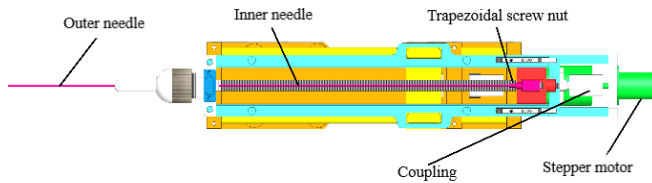


Fig. 4 Top view of the assembly.

The External Needle Insertion Mechanism (Part 1): The outer needle is fixed on the inner needle slide, the inner needle slide and the ball screw slide are fixed, and then the servo motor is used as the power source to drive the inner needle slide and the outer needle together. The advantage is that the accuracy of the outer needle feeding is ensured, and the device is compact.

The Automatic Particle Placement Mechanism (Part 2): Fig. 5 shows an exploded view of the automatic particle-discharging mechanism. The cylindrical drug particles are placed in a "medicine grain storage tank", and the compression spring supplies the pressure of the pressure plate to press the medicine particles, and then the inner needle is inserted from the drug-oriented. A particle is pushed into the outer needle core, and the particle is pushed to the tumor cell, and then the inner needle is pulled out, and a row of particles is pressed under the pressure of the pressure plate. A particle is pressed into the drug-oriented, and then the inner needle is again inserted into the drug-oriented to push away the particle, and thus repeat this procedure, the repeated injection of the particle is completed.

The Internal Needle Repeated Injection Mechanism (Part 3): The movement of the inner needle is a uniform linear reciprocating motion, and the mechanic stroke is fixed. We chose a deceleration stepping motor to provide driving source. The inner needle is mounted on the slider fixed to the nut, and the trapezoidal screw nut drive is adopted to realize the reciprocating linear motion of the inner needle.

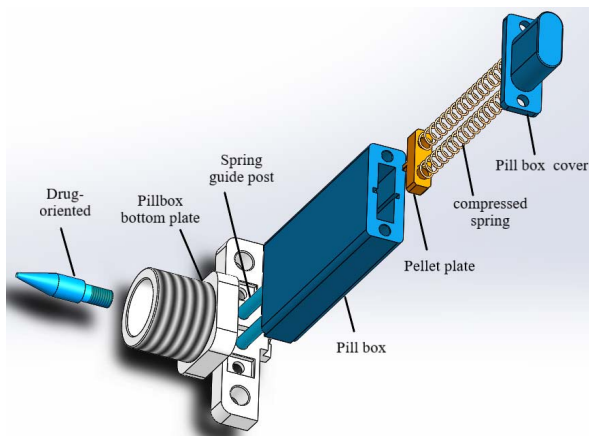


Fig. 5 Exploded view of the automatic particle placement mechanism.

C. Structural Optimization

Stable Support Design for Inner Needle Slide: Considering the inner needle slide length which is equal to the length of the inner needle is too large, we add a support mechanism with micro-bearing to increase the stability of the inner needle movement, as shown in Fig. 6. Two pairs of micro-bearings are mounted on the left support plate and the middle support plate, respectively, and the two ends of the bearing shaft are processed into a D-shaped shaft, and the fixing of the bearing shaft is completed by fixing the two ends of the top wire.

D. Structural Innovation

Easy to Disassemble Design: As shown in Fig. 3, the inner needle moving part is fixed to the ball screw slide by two screws. This device is easy to disassemble and can be used one-off because of the low cost of the inner needle movement part. In addition, the nut-fixing mode of the outer needle allows the outer needle to be replaced without tools such as a wrench, which is convenient for the operator.

Tooling Design: Considering the size of the granules is $\phi 0.8$, it is very difficult to distribute the granules in a row in the storage tank without the aid of tools. Therefore, the granule arrangement auxiliary tool is designed, as shown in Fig. 7. The tool consists of two parts, the inner core and the outer casing, all of them are manufactured by 3D printing. The particle is clamped at the bottom end of the inner core, and the particles are sent into the bottom of the storage tank. Then, we push the shell down to push the particle from the pinch end to complete the granule arrangement.

The Design of Automatic Particle Placement Mechanism: The reasonable structural design makes the automatic particle placement mechanism safe and reliable, and also makes the device smaller and more compact.

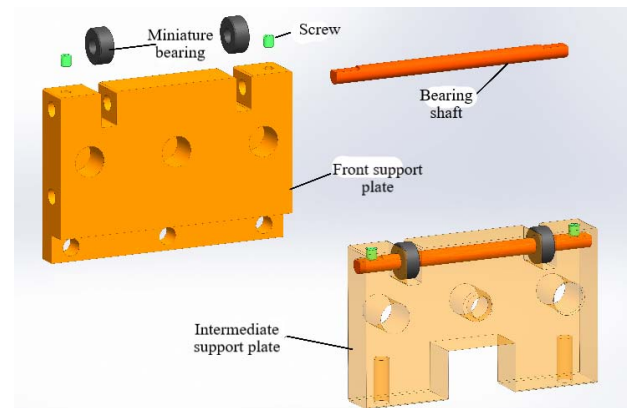


Fig. 6 Schematic diagram of inner needle slide support structure

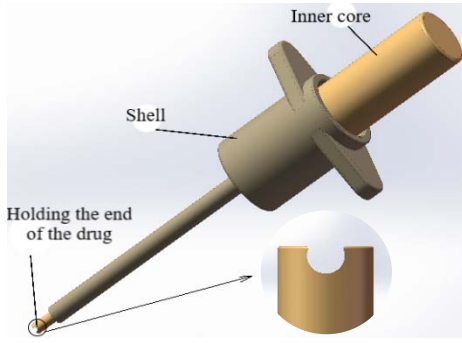


Fig. 7 The granule arrangement auxiliary tool.

III. STRUCTURAL STRENGTH CHECK

A. Checking the axis of the ball screw

According to the lateral movement stroke of 100 mm, the maximum distance between the two fixed supports is calculated using (1):

$$L \approx (1.1 \sim 1.2) \cdot l + (10 \sim 14) \cdot P_n = 134 \text{ mm} \quad (1)$$

According to the screw installation method, the axial ends are fixed, and the screw thread bottom diameter is:

$$d_{2m} \geq 0.039 \sqrt{\frac{F_o L}{1000 \delta_m}} \quad (2)$$

F_o represents static friction of the guide rail, taking it as 5.024 N. L is the maximum distance from the ball nut to the fixed end of the ball screw, taking L as 134 mm.

According to (2):

$$d_{2m} \geq 0.039 \times \sqrt{\frac{5.024 \times 134}{1000 \times 0.02}} = 0.226 \text{ mm} \quad (3)$$

We take the ball screw shaft nominal diameter as 6 mm, which meets the strength requirements.

B. Checking the Axis of the Lead Screw

Calculate the diameter of the thread under the condition of wear resistance. For the trapezoidal and rectangular thread the diameter is:

$$d_2 \geq 0.8 \sqrt{\frac{F}{\psi [P]}} \quad (4)$$

F is axial load of the helix, and ψ is a factor selected according to the nut structure.

$[P]$ represents allowable pressure of sliding spiral pair material

If it is a one-piece nut, the clearance cannot be adjusted after wear, in this case, take ψ as 1.2 ~ 2.5.

The axial load F of the spiral in this project is 1 N. The ψ is chosen to be 1.5. The allowable pressure $[P]$ obtained from the spiral pair material is 6 ~ 8 MPa, taking it as 7 MPa. Then the diameter of the thread obtained from (4) is:

$$d_2 \geq 0.8 \sqrt{\frac{1}{7 \times 10^6 \times 1.5}} = 0.2469 \text{ mm} \quad (5)$$

Taking the nominal diameter of the trapezoidal screw shaft d as 6 mm, it is evident that the thread diameter d_2 is 0.2496 mm.

IV. CONTROL SYSTEM DESIGN

A. Introduction to The Function of the Control System

The functions of the control system include external needle movement limit, control of the outer needle for a given speed, a given depth of motion, the control of the inner needle feed speed, the reciprocating motion of the fixed stroke, and one-button emergency stop function, etc. Besides, positioning accuracy of ± 0.5 mm and repeatability of ± 0.1 mm are required.

B. Control System Hardware Design

In order to meet the functional requirements of the control system, we designed the hardware system including encoder, servo motor driver, stepper motor driver, photoelectric sensor switch, magnetic switch, USB-CAN, 24V DC power supply and so on. Fig. 8 are the interface figures of servo motor driver and stepper motor driver. The hardware connection diagram of the control system is shown in Fig. 9.

C. Introduction to The Software of the Control System

Since the servo driver selected by the device supports the CAN protocol, the servo operation management system software using the servo driver can use the USB to CAN to connect the host computer and the driver, and the command of the software uses the ASCII command. Furthermore, it has a one-to-one correspondence with the CAN command, so it can be controlled with a simple ASCII command without sending a CAN command.

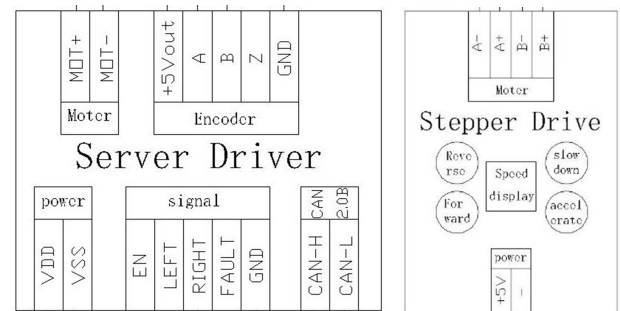


Fig. 8 the interface figures of servo motor driver and stepper motor driver.

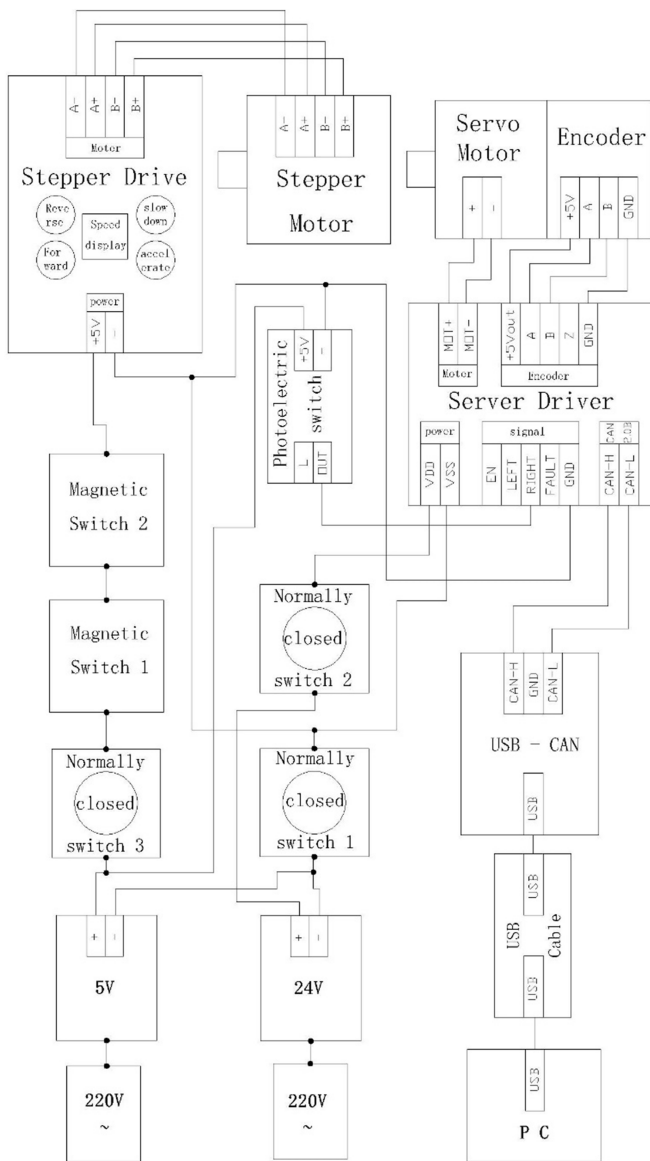


Fig. 9 Hardware wiring diagram.

V. PHYSICAL ASSEMBLY AND EXPERIMENT

Figs. 10 shows a physical diagram of a close-range radiotherapy particle implantation device. After the assembly and debugging, the verification experiment is performed.

The accuracy test of the device is measured by a laser tracker with a measurement accuracy of 0.01 mm, and the

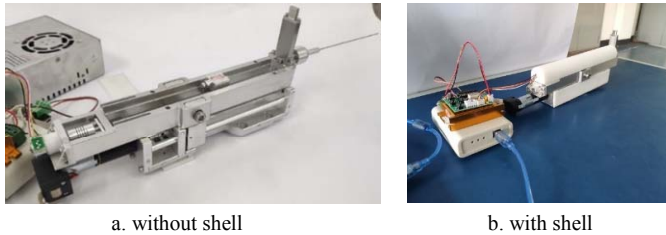


Fig. 10 Physical display of the device

measurement site is shown in Figure 11. Three sets of data were collected during the measurement process, which were used to measure the absolute position accuracy (positioning accuracy) of the outer needle feed, the displacement increment accuracy of 5 mm, and the repeat positioning accuracy. During the measurement process, the amount of change in the displacement of the laser tracker in the X-axis direction is the amount of change in the displacement of the outer needle. Specific data and analysis are given below.

Table 1 shows the data obtained when measuring the outer needle's positioning accuracy of the device. The measurement process is as follows: first, measure the spatial coordinates when the absolute position of the outer needle is 0, and then give an instruction of the absolute position of the outer needle of 10 mm and measure the spatial coordinate. Then give the command that the absolute position of the outer needle is 0 to return to the 0 position, and then give the command of the outer needle absolute position of 20 mm and measure its spatial coordinates. Repeat the measurement like this until a given absolute position of 90 mm, and a total of 9 sets of data are obtained. After data analysis, it can be concluded that the positioning accuracy of the outer needle of the device is within ± 0.5 mm.

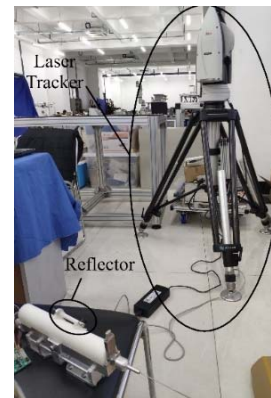


Fig. 11 Measurement site

Table 2 shows the data obtained when measuring the 5mm displacement increment of the outer needle of the device. The measurement process is as follows: first, give the outer needle absolute position command 0 to make it at the 0 position, then give the outer needle absolute position 5mm command and measure its spatial coordinates. Then give the instruction of the absolute position of the outer needle 10 mm again and measure its spatial coordinates. In this way, an absolute position

TABLE I

ABSOLUTE POSITIONAL ACCURACY DATA STATISTICS

the Coordinates When Depth is 0	Given Depth /mm	Actual Arrival Position Coordinates			Actual Depth /mm	error /mm
		X /mm	Y /mm	Z /mm		
X=296.27 mm	10.00	306.41	-1788.32	-723.74	10.14	0.14
	20.00	316.39	-1789.36	-723.72	20.12	0.12
	30.00	326.45	-1789.34	-723.76	30.18	0.18
	40.00	336.39	-1790.28	-723.75	40.12	0.12
Y=-1788.31 mm	50.00	346.43	-1790.38	-723.79	50.16	0.16
	60.00	356.48	-1791.20	-723.71	60.21	0.21
Z=-723.75 mm	70.00	366.44	-1790.19	-723.72	70.17	0.17
	80.00	376.55	-1792.15	-724.76	80.28	0.28
	90.00	386.57	-1792.28	-725.69	90.30	0.30

TABLE II

5mm DISPLACEMENT INCREMENT DATA STATISTICS

Given Depth /mm	Actual Arrival Position Coordinates			Actual Depth /mm	Absolute error /mm	Actual Displacement Increment /mm	Incremental error /mm
	X /mm	Y /mm	Z /mm				
5.00	301.38	-1788.29	-723.73	5.11	0.11	5.11	0.11
10.00	306.45	-1788.25	-723.76	10.18	0.18	5.07	0.07
15.00	311.54	-1788.21	-723.77	15.27	0.27	5.09	0.09
20.00	316.66	-1788.26	-723.75	20.39	0.39	5.12	0.12
25.00	321.75	-1788.31	-723.74	25.48	0.48	5.09	0.09
30.00	326.89	-1788.34	-723.73	30.62	0.62	5.14	0.14
35.00	331.99	-1788.39	-723.70	35.72	0.72	5.10	0.10
40.00	337.08	-1788.41	-723.74	40.81	0.81	5.09	0.09
45.00	342.18	-1788.40	-723.76	45.91	0.91	5.10	0.10
50.00	347.31	-1788.35	-723.78	51.04	1.04	5.13	0.13
55.00	352.40	-1788.32	-723.81	56.13	1.13	5.09	0.09
60.00	357.50	-1788.31	-723.76	61.23	1.23	5.10	0.10

command of 5 mm is added every time until the given absolute position is 60 mm, and a total of 12 sets of data are obtained. After data analysis, it can be seen that the accuracy of the 5mm displacement increment of the outer needle of the device is within ± 0.15 mm.

Table 3 shows the data obtained when measuring the outer needle's repeat positioning accuracy of the device. The measurement process is as follows: first, the absolute position command of the outer needle is set to 0 to be in the 0 position, then the command of the outer needle absolute position of 10 mm is given and the spatial coordinate is measured. Then give the command that the absolute position of the outer needle is 0 to return to the 0 position, and then give the command of the absolute position of the outer needle 10 mm and measure its spatial coordinates. The spatial coordinates when the absolute position is 10 mm are measured five times in this way. A total of 5 sets of data were obtained. Similarly, the spatial coordinates of the absolute position of 30 mm are measured again five times. After data analysis, it can be concluded that the repeatability of the device is within ± 0.1 mm.

TABLE III

Repeat positioning accuracy data statistics

Given Depth /mm	Actual Arrival Position Coordinates			Maximum Difference /mm	Repeated Positioning Accuracy /mm
10.00	307.77	-1788.43	-724.29	0.11	±0.055
10.00	307.71	-1788.47	-724.24		
10.00	307.70	-1788.50	-724.24		
10.00	307.67	-1788.49	-724.23		
10.00	307.66	-1788.52	-724.22		
30.00	327.86	-1789.50	-724.23	0.08	
30.00	327.83	-1789.52	-724.21		
30.00	327.80	-1789.53	-724.19		
30.00	327.79	-1789.54	-724.17		
30.00	327.78	-1789.53	-723.17		

VI. INNOVATION AND CONCLUSION

The particle implantation device is with two degree of freedom, which makes the device more flexible, and no longer requires the mechanical arm to complete the outer needle-punching movement. the nut-fixing mode of the outer needle allows the outer needle to be replaced without tools such as a wrench, which is convenient for the operator. The specially designed automatic particle filling mechanism stores 40 particles, which can realize the automatic filling of the granules. It is stable and reliable, and its compacted design can also reduce the radiation of radioactive particles. The inner needle movement adopts the screw nut transmission to make the device compact and optimize the structure of the device. The outer needle movement adopts the ball screw drive and the servo motor drive to ensure the precision of the outer needle.

In general, the design of the device solves the problem of continuous and automatic filling of particle. The transmission mode of the screw nut makes the structure of the device compact and reasonable, the accuracy of the outer needle is high, and the quick-release design of the moving part of the inner needle and the quick change design of the outer needle allows the doctor to quickly remove the inner and outer needles during the procedure. The design of the device has great reference significance for the prototype design of close-range radiotherapy particle implantation equipment.

REFERENCES

- [1] J. L. Raytis, B. E. Yuh, C. S. Lau, Y. Fong, and M. W. Lew, "Anesthetic implications of robotically assisted surgery with the da Vinci Xi surgical robot," *Open Journal of Anesthesiology*, vol.6, no.08, pp.115, 2016.
- [2] N. Goyal, F. Yoo, D. Setabutr, and D. Goldenberg, "Surgical anatomy of the supraglottic larynx using the da Vinci robot," *Head & neck*, vol.36, no.8, pp.1126-1131, 2014.
- [3] A. Sánchez, P. Poignet, E. Dombre, A. Menciassi, and P. Dario, "A design framework for surgical robots: Example of the Araknes robot controller," *Robotics and Autonomous Systems*, vol.62, no.9, pp.1342-1352, 2014.

- [4] M. E. Rentschler, and D. Oleynikov, "Recent in vivo surgical robot and mechanism developments," *Surgical endoscopy*, vol.21, no.9, pp.1477-1481, 2007.
- [5] A. Jemal, R. Siegel, and E. Ward. "Cancer statistics," *CA: a cancer journal for clinicians*, vol.58, no.02, pp.71-96, 2008.
- [6] S. Hassfeld, J. Muhling, "Computer assisted oral and maxillofacial surgery-a review and an assessment of technology," *International Journal of oral and maxillofacial surgery*, vol.30, no.01, pp.2-13, 2001.
- [7] T. R. K. Varma, P. Eldridge, "Use of the NeuroMate stereotactic robot in a frameless mode for functional neurosurgery," *The International Journal of Medical Robots and Computer Assisted Surgery*, vol.2, no.02, pp.107-113, 2006.
- [8] S. Saito, H. Nagata, and M. Kosugi, "Brachytherapy with permanent seed implantation," *International journal of clinical oncology*, vol.12, no.06, pp.395-407, 2007.
- [9] M. Arand, E. Hartwig, and L. Kinzl, "Spinal navigation in cervical fractures —A preliminary clinical study on J udet-osteosyn-thesis of the axis," *Computer Aided Surgery*, vol.6, pp.170-175, 2001.
- [10] L. P. Nolte, M. A. Slomczykowski, and U. Berlemann, "A new approach to computer aided spine surgery: fluoroscopy-based surgical navigation," *EuroSpine Journal*, vol.9, pp.78-88, 2000.
- [11] M. J. H. Lum, D. C. W. Friedman, "The Raven: Design and validation of a telesurgery ststem," *The International Journal of Robotics Research*, vol.28, no.09, pp.1183-1197, 2009.
- [12] J. Hong, T. Dohi, and M. Hashizume, "An Ultrasound-driven Needle Insertion Robot for Percutaneous," *Institute of Physics Publishing*, vol.49, no.03, pp.441-445, 2003.
- [13] W. T. Luo, "Primary clinical investigation of ultrasound-guide interstitial implantation of ¹²⁵I radioactive seeds for brachytherapy of recurrent oral and maxillofacial malignancies", Shijiazhuang: Hebei Medicine University, 2014(in Chinese).
- [14] K. C. Olds, P. Chalasani and P. Pacheco-Lopez, "Preliminary evaluation of a new microsurgical robotic system for head and neck surgery" [C]// Proceedings of IEEE/RSJ International Conference on Intelligent Robots and Systems, Chicago, IL, USA: IEEE, 2014: 1276—128
- [15] X. F. Wang, "Structural design and simulation of 1P2R prostate biopsy robot", Harbin: Harbin University of Science and Technology, 2014(in Chinese).
- [16] X. G. Duan, N. N. Chen and Y. G. Wang, "Design and implementation of radioactive particle implantation robot for craniomaxillofacial tumor", Beijing: Beijing Institute of Technology, 2017(in Chinese).
- [17] X. Z. Kong, "Research on key technology of craniomaxillofacial puncture diagnosis and treatment robot", Beijing: Beijing Institute of Technology, 2015(in Chinese)